Int J Adv Manuf Technol
DOI 10.1007/s00170-013-5276-3

ORIGINAL ARTICLE

Deformation measurement of circular steel plates using projected fringes

Kjell J. Gåsvik · Kjell G. Robbersmyr · Trond Vadseth · Hamid Reza Karimi

Received: 6 June 2013 / Accepted: 25 August 2013

Abstract Fringe projection is a versatile method for mapping the surface topography. In this paper, it is used to measure the deformation of steel plates under static penetration. Here, the surface shape changes continuously. Therefore, it is important to minimize the registration time. To achieve this, we apply a method of fringe location with subpixel accuracy that requires only a single exposure for each registration. This is in contrast to phase shifting techniques that require at least three separate exposures.

Keywords Fringe projection · Optical measurements · Steel plates

1 Introduction

Projected fringes is a full field method for mapping the topography of surfaces [1–5]. It consists of imaging the fringes projected onto the surface with subsequent processing of the fringe data. In recent years, it has been combined with phase shift techniques [6–12] or Fourier transform methods [13–18]. With some exceptions [19, 20], reports from work with these methods are done inside the optical laboratory. Recently, the authors in [21] have developed an optical measurement system to measure surface profile and three-dimensional deformation of small objects simultaneously, by a combination of fringe projection and a two-dimensional digital image correlation technique. Moreover, a Monte Carlo-based uncertainty approach is proposed to estimate overall error in fringe projection in [22].

In this paper, we describe an intensity method based on location of the fringe positions with subpixel accuracy by means of a zero-crossing algorithm. This method is applied to the measurement of deformations of steel plates under static penetration. Since the deformation increases continuously, it is important to have the exposure time as short as possible. The phase shift methods require at least three separate exposures of each deformation state and therefore become inadequate for recording fast dynamic events. The contributions of this article are mainly twofold: (1) a method for full field measurement of the dynamic deformation of steel plates is presented; (2) the experimental results are successfully carried out in mapping the development of the plate deformation.

The remainder of this paper is organized as follows: in Section 2, the measuring system using fringe projection methodology is described. Section 3 presents the test description and a detailed discussion on experimental results is given and we conclude the paper with Section 4.

2 System description

The measuring principle is illustrated in Fig. 1. A grating is projected onto the surface at an angle θ_0 to the z axis. A charged coupled device (CCD) camera points along the z axis and images the surface with the superposed grating lines. When the object surface deviate from the reference surface, e.g., the xy plane, a projected grating line will be displaced laterally at distance Δu as seen by the camera.

K. J. Gåsvik
Spectra Vision AS, Fernanda Nissens vei 15, 7046 Trondheim, Norway

K. G. Robbersmyr (✉) · H. R. Karimi
Department of Engineering, Faculty of Engineering and Science, University of Agder, 4886 Grimstad, Norway
e-mail: kjell.g.robbersmyr@uia.no

H. R. Karimi
e-mail: hamid.r.karimi@uia.no

T. Vadseth
Division of Safety and Reliability, SINTEF, 7465 Trondheim, Norway

Published online: 07 September 2013

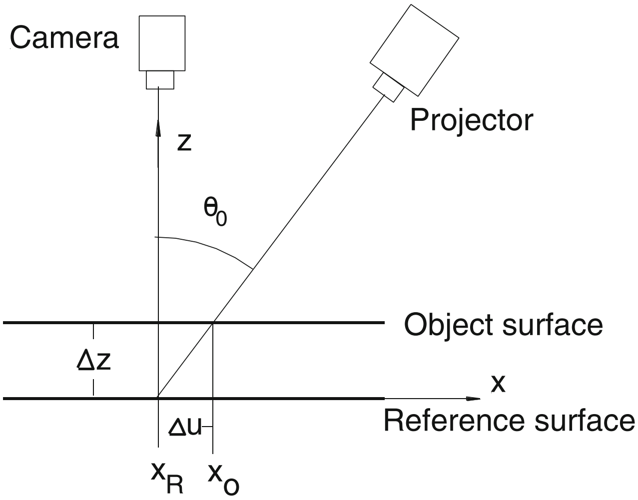

Fig. 1 The measuring principle

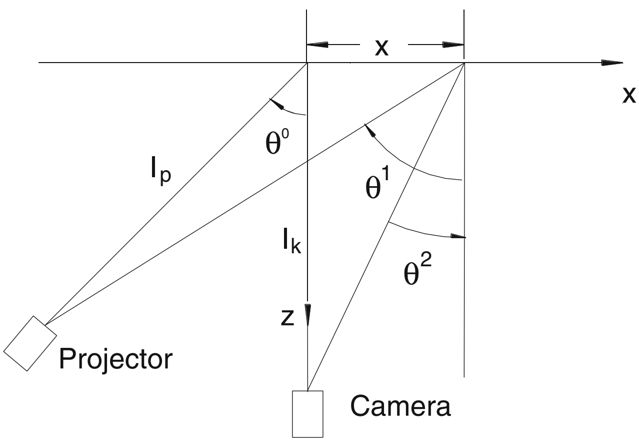

Fig. 2 Fringe projection geometry

The relation between Δu and the corresponding surface deviation Δz is given by

$$\Delta z = \frac{x_0 - x_R}{\tan\theta_0} = \frac{\Delta u}{\tan\theta_0} \tag{1}$$

where x_R and x_0 denote the fringe positions on the reference surface and on the object surface, respectively.

When imaging a grating of period d_g, the fringe period on the surface is given by

$$d_{x0} = m_p \frac{d_g}{\cos\theta_0} \tag{2}$$

where m_p is the magnification of the projection unit. When putting $\Delta u = d_{x0}$, the surface deviation per fringe is given by

$$\Delta z(per\ fringe) = \frac{m_p d_g}{\sin\theta_0} \tag{3}$$

As the measuring point moves along the object surface, Fig. 2, the relation between the surface deviation Δz and the fringe displacement becomes more complicated [1, p. 234]:

$$\Delta z(x) = \cos\theta_0 \left[\sin\theta_0 + \frac{(l_k - l_p\cos\theta_0)x}{l_k l_p}\right]^{-1} \cdot \Delta u(x) \tag{4}$$

where l_k is the distance between the camera lens and the coordinate center and l_p denotes the distance between the projector lens and the coordinate center.

The relation given in Eq. (4) can be written as

$$\Delta z(x) = S(\theta_0, l_k, l_p, x) \cdot \Delta u(x) \tag{5}$$

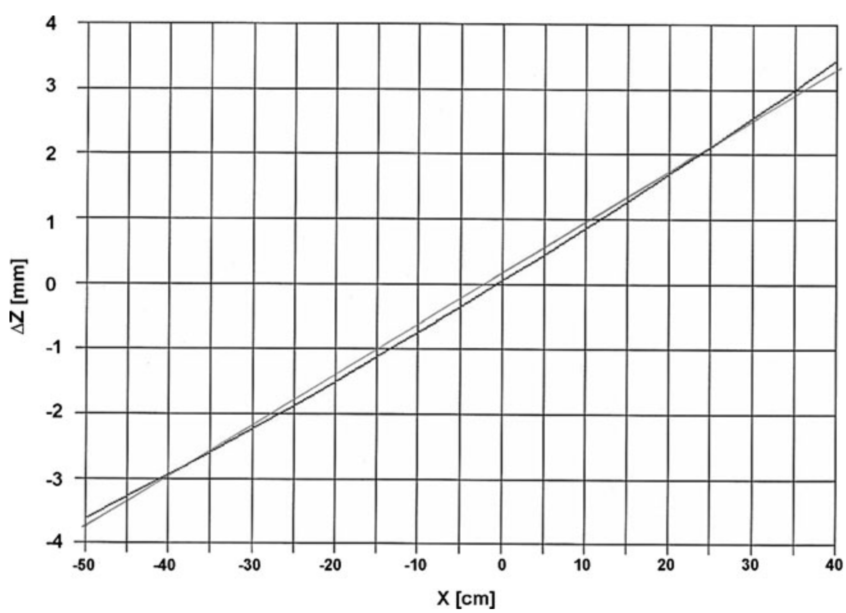

Fig. 3 Result from measurement of a rotation of a plane. *Thick curve* the measurement; *thin curve* the ideal straight line

where

$$S(\theta_0, l_k, l_p, x) = \cos\theta_0 \left[\sin\theta_0 + \frac{(l_k - l_p \cos\theta_0)x}{l_k l_p} \right]^{-1} \tag{6}$$

is a system function determined by the geometry of the experimental setup. Notice when the camera and the projector are located at the same height above the reference surface ($l_k - l_p \cos\theta_0 = 0$), S becomes equal to $1/\tan\theta_0$, i.e., independent of x.

Another reason for not using phase shifting techniques is pointed out by [4] and [10]. Divergent illumination introduces a nonlinear phase into the fringe function. While the system function S in Eq. (6) can be made linear by making $l_k - l_p \cos\theta_0 = 0$, the phase $\psi(x) = u(x)/d_x$ where d_x is the fringe pitch which is given by

$$d_x = \frac{1}{f_0} \left[1 + \frac{x \sin\theta_0}{l_p} \right]^2 \tag{7}$$

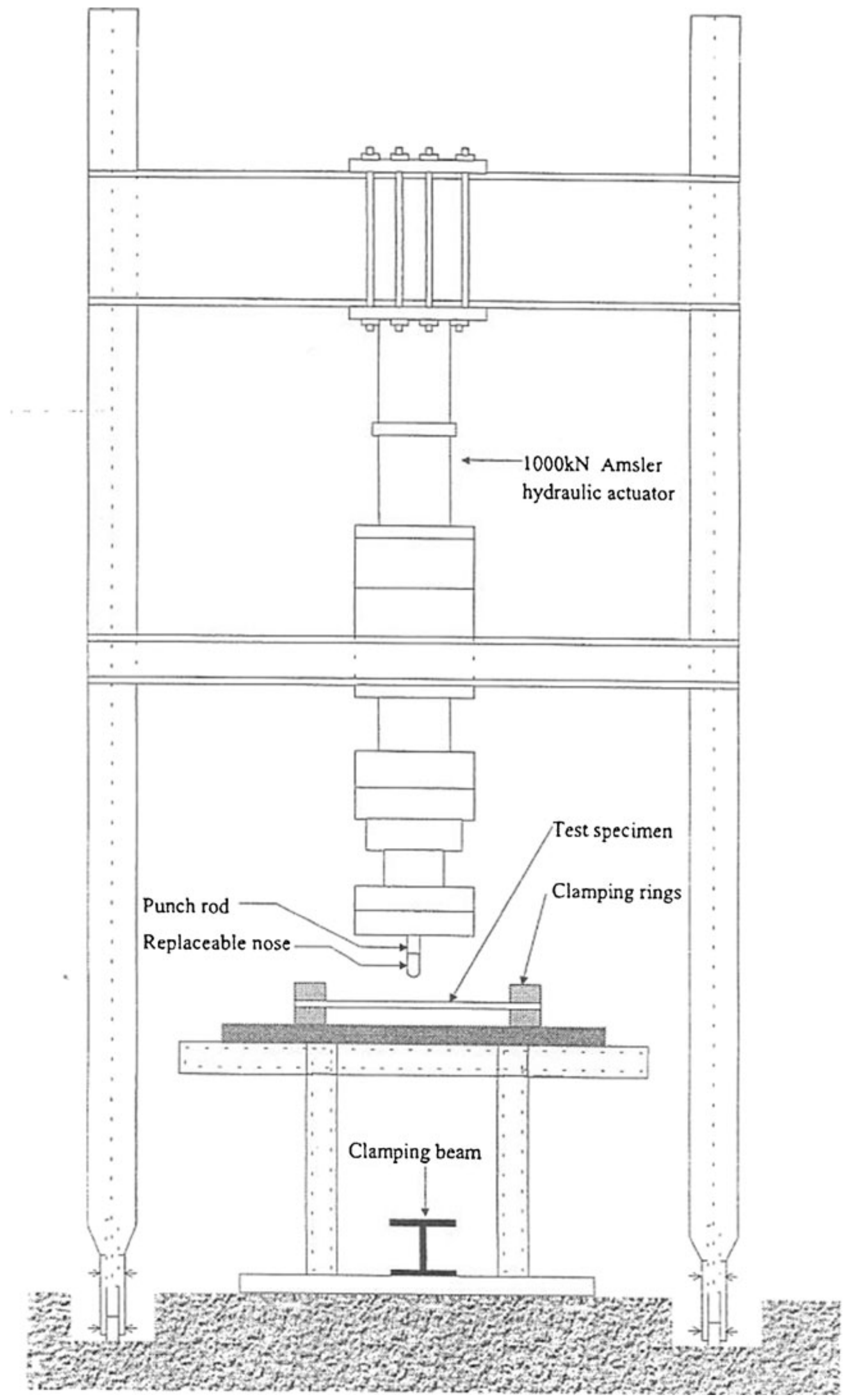

Fig. 4 The test rig

Here, f_0 is the fringe frequency in the xy plane for $x=0$, see Eqs. (7.35) and (7.43) of [1]. This results in a phase function with a quadratic dependence on x and cannot be eliminated unless $l_p \to \infty$, i.e., plane wave illumination.

The measurement accuracy is dependent on the accuracy with which the fringe positions are detected. This is done by a zero-crossing algorithm described in [1, p. 274]. By this algorithm, the fringe positions are located with subpixel accuracy [23].

When the fringe positions in both the object and reference image are located, the measuring system determines Δu and calculates Δz according to Eq. (4). To do this, the mutual fringe order on the reference and the object must be found. In the general case, the zero-order fringe must be pointed out manually. In the present application, the calculations start at the clamped edge of the steel plate where $\Delta u=0$. The measurement algorithm therefore starts automatically without manual assistance. The calculated $\Delta z(x)$ is stored in computer memory. The results can be displayed either as a gray-scale level picture or as a contour map.

A simple and reliable test of this system is to image a plane surface before and after a known tilt. Figure 3 shows the result of such a test. A plane surface of about 1 m^2 is imaged before and after a rotation angle of about 8 millirad about the vertical axis. From the smoothness of the measured curve, we can conclude that the zero-crossing algorithm works properly. Also, the ideal straight line in the diagram is drawn. The deviation from this line is seen to be less than about 0.1 mm. This deviation is mainly due to small errors in the setup parameters resulting in a minor error in the system function. It should be noted that the projected fringes in this test had the highest possible quality. One cannot expect such a small measuring error on, e.g., steel plates, but the results of our project indicate a measuring error of about 0.2 mm.

3 Test description

The present work was part of a project of testing the behavior of Weldox steel plates under static penetration. Weldox is a trade name of a general structural steel with a high-yield strength. The experimental setup is shown in Fig. 4. The test rig was an Amsler 1,000 tons jack with a length span of ±100 mm. The circular steel plates were mounted by clamping rings at the circumference and the load was applied at the center by a punch rod. The load was applied slowly but continuously and measured by a force sensor. The movement of the punch road was monitored by both a laser distance meter and an inductive probe. The loading stopped automatically when the steel plate was penetrated. Five different model parameters were used including plate thickness, geometry of the replaceable nose, rod diameter, mounting conditions,

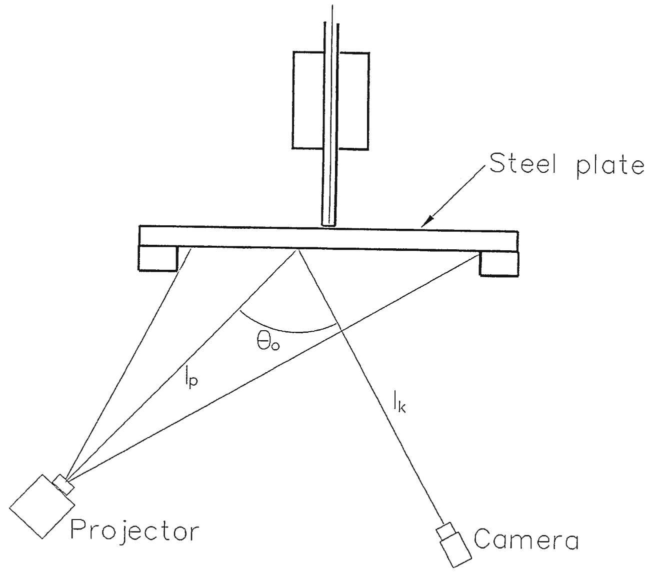

Fig. 5 The experimental setup

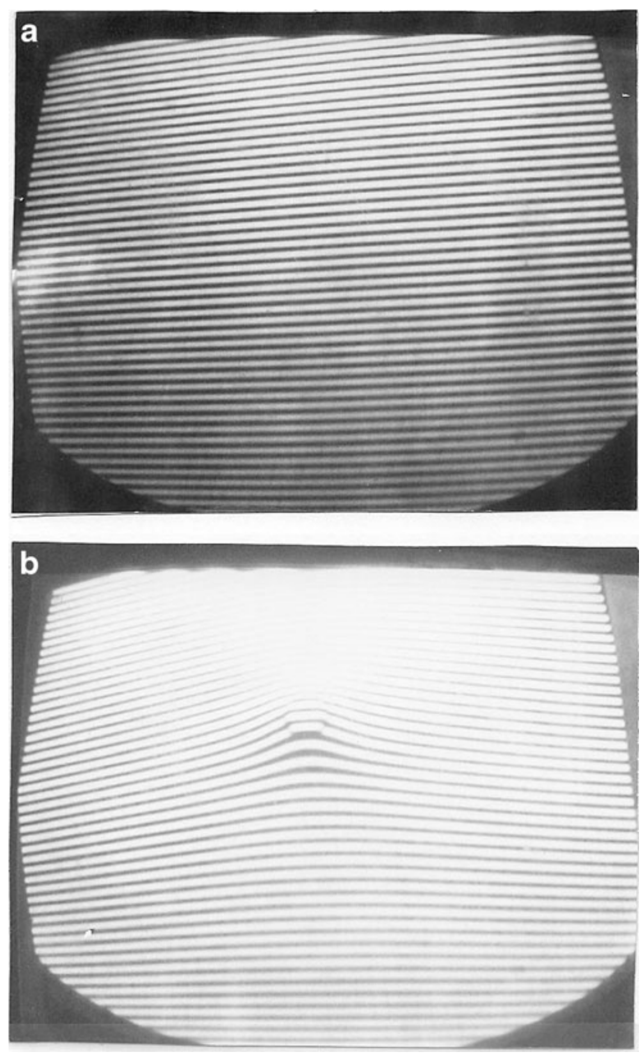

Fig. 6 **a** The projected fringes on a plate just before applying the load, **b** the fringes on the same plate just before penetration

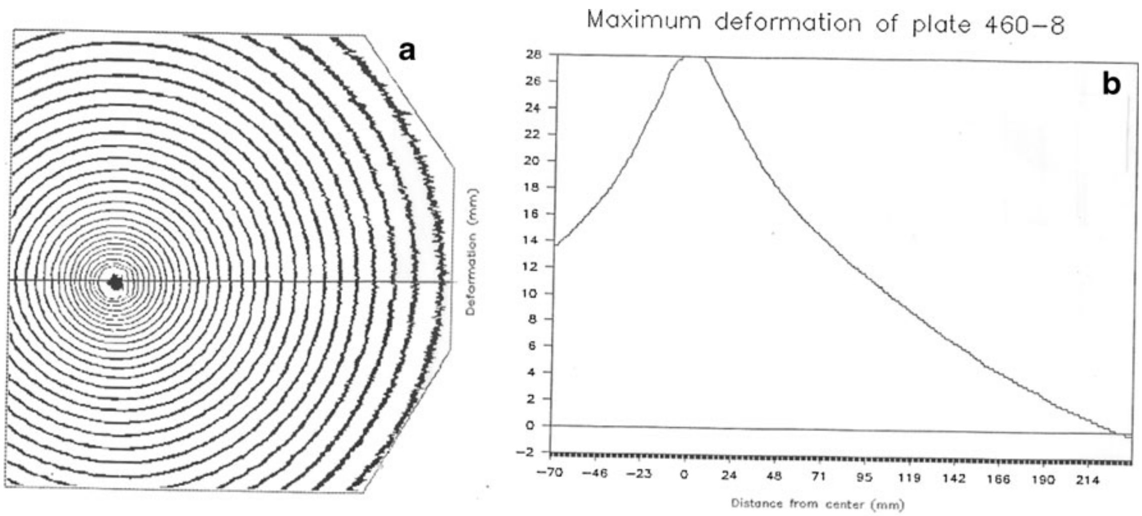

Fig. 7 **a** The deformation of the imaged part of the plate displayed as a contour map, **b** the deformation along a radial line for the same plate

and material quality. By varying these parameters, this test could give valuable information about the behavior of steel plates under static penetration.

Here, we will not go into details of the different findings of the project, but rather present the measuring method used to map the surface profile of the steel plates as the force increased.

3.1 Experimental set up for the fringe projection system

Figure 5 shows the experimental setup. The circular steel plate (radius, 250 mm) is supported along its rim by a circular frame. It is loaded at its center by a pin (cross section, 1 cm^2) driven by a hydraulic system. The pin moves slowly downward resulting in an increasing deformation, and finally, the pin penetrates the steel plate. The time lapse from initiating the load to the penetration will among other things depend on the thickness and quality of the steel plate. In our experiments, it lasted typically between 5 and 15 min.

The purpose of the present experiment was to map the plate deformation as a function of the applied load. The projected fringes imaged by the camera were therefore grabbed and stored in the computer each 20th second. At the same instant, the load read off by a force sensor was registered and filed.

The optical system consists of a projector (550 W Xenon lamp) with a grating (4 lines/mm) and a CCD camera

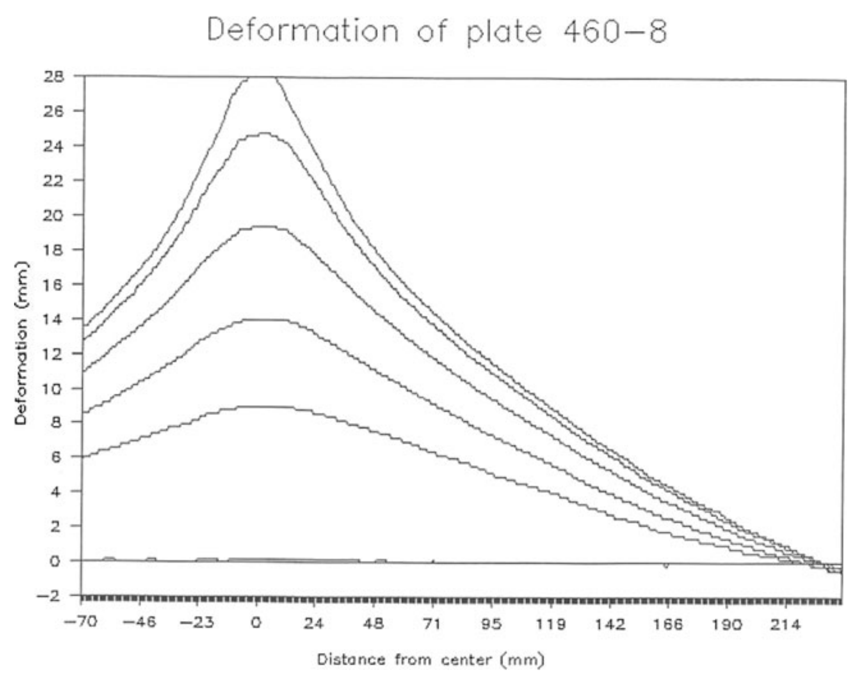

Fig. 8 The deformation along a radial line plotted at different stages of the plate deformation

connected to a frame grabber card inside a PC. To get high contrast of the projected fringes, the steel plate was painted white. The system has the following geometric configuration:

Distance, projector–steel plate: l_p=910 mm
Distance, camera–steel plate: l_c=735 mm
Projection angle: θ_0=53°
Focal length of camera lens: f=10 mm

Since the deformation is centrally symmetric, we need not measure the whole plate area. The length of the imaged area therefore covered about ¾ of the diameter.

The first stored image of a measuring sequence was grabbed just before the load was applied. This initial image served as the reference for the subsequent images in the same sequence. After finishing a sequence (i.e., after penetration of the plate), we therefore could map the deformation of the plate as it develops in steps of 20 s.

3.2 Experimental results

Figure 6a shows the projected fringes on a plate just before applying the load, while Fig. 6b shows the fringes on the same plate just before penetration. Figure 7a shows the deformation of the imaged part of the plate displayed as a contour map. Figure 7b shows the deformation along a radial line for the same plate.

In Fig. 8, the deformation along a radial line is plotted at different stages of the plate deformation. From this plots, one can see how the deformation develops as a function of time (i.e., load). In this project, 17 different steel plates of different steel plate quality and thickness were measured.

4 Conclusion

A method for full field measurement of the dynamic deformation of steel plates is presented. The experimental results were successful in mapping the development of the plate deformation. The only problem was that the white paint teared off just before penetration for some of the plates.

Although the dynamic development in this case was comparatively slow, the experiments have shown that this system is capable of measuring dynamic events at the same speed as the frame rate of the camera. With phase-shift methods, it is common to use four exposures for each surface state, making it at least four times as slow as our method. Future work will investigate on analysis of the measurements based on uncertainty on fringe projection technique and reduction of the noise in the measurements.

References

1. Gåsvik KJ (2002) Optical metrology, 3rd edn. Wiley, Chichester. ISBN 0-470-84300-4
2. Sciammarella C, Lamberti L, Boccaccio A (2008) General model for moiré contouring, part 1: theory. Opt Eng. doi:10.1117/1.2899039
3. Chen F, Brown GM, Song M (2000) Overview of three-dimensional shape measurement using optical methods. Opt Eng 39(1):10–22
4. Wang Z, Du H, Bi H (2006) Out-of-plane shape determination in generalized fringe projection profilometry. Opt Express 14:12122–12133
5. Huntley J M, Ogundana T, Borguete R L, Coggrave C R (2002) Large-scale full-field metrology using projected fringes: some challenges and solutions. 2007 SPIE. Vol 6616
6. Jeong M.-S, Kim S.-W (2001) Phase-shifting projection moiré for out-of-plane displacement measurement. Second International Conference on Experimental Mechanics, Proc. SPIE, vol. 4317, p. 170–179.
7. Yoshizawa T, Tomosawa T (1993) Shadow moiré topography by means of phase-shift method. Opt Eng 32(7):1668–1674
8. Rosvold GO (1990) Fast measurement of phase using a PC-based frame grabber and phase stepping technique. Appl Opt 29:237–241
9. Huang P, Chiang F P (1999) Recent advances in fringe projection technique for 3D shape measurement, SPIE conference on optical diagnostics for fluids/heat/combustion and photomechanics for solids. Colorado, SPIE Vol 3783
10. Chen L, Quan C (2005) Fringe projection profilometry with nonparallel illumination: a least-squares approach. Opt Let 30(16): 2101–2103
11. Sansoni G, Trebeschi M, Docchio F (2006) Fast 3 D profilometer based upon the projection of a single fringe pattern and absolute calibration. Meas Sci Tech 17:1757–1766
12. Huang P, Zhang S, Chiang F P (2005) Trapezoidal phase shifting for three-dimensional shape measurement. Opt Eng 44(12), 123601. doi: 10.1117/1.2147311
13. Takeda M, Ina H, Kobayashi S (1982) Fourier-transform method of fringe-pattern analysis for computer-based topography and interferometry. J Opt Soc Am 72(1):156–160
14. Takeda M, Mutoh K (1983) Fourier transform profilometry for the automatic measurement of 3-D object shape. Appl Opt 24:3977–3982
15. Sciammarella C, Lamberti L, Sciammarella FM (2005) High-accuracy contouring using projection moiré. Opt Eng 44(9):093605
16. Salas L, Luna E, Salinas J, Garcia V (2003) Profilometry by fringe projection. Opt Eng 42:3307–3314
17. Malcom A A, Burton D R, Lalor M J (1990) Full-field Fourier fringe analysis for industrial inspection. 1990 SPIE
18. Sciammarella C, Lamberti L, Boccaccio A, Cosola E, Posa D (2008) General model for moiré contouring, part 2: applications. Opt Eng 47(3):033606
19. Gasvik KJ, Robbersmyr KG, Vadseth T (2010) Projected fringes for the measurement of large aluminum ingots. Meas Sci Technol 21:105302
20. Spagnolo GS, Guttari G, Sapia C, Ambrosini D, Paoletti D, Accardo G (2000) Contouring of artwork surface by fringe projection and FFT analysis. Opt Lasers Eng 33:141–156
21. Shi H, Ji H, Yang G, He X (2013) Shape and deformation measurement system by combining fringe projection and digital image correlation. Optic Laser Eng 51(1):47–53
22. Molimard J, Navarro L (2013) Uncertainty on fringe projection technique: a Monte-Carlo-based approach. Optic Laser Eng 51(7): 840–847
23. Gåsvik KJ, Robbersmyr KG (1994) Error analysis of a zero-crossing algorithm for fringe location. Opt Eng 33:246–250